Modified Numerical Modeling of Axially Loaded Concrete-Filled Steel Circular-Tube Columns

Phu-Cuong Nguyen
Advanced Structural Engineering Laboratory
Faculty of Civil Engineering
Ho Chi Minh City Open University
Ho Chi Minh City, Vietnam
cuong.pn@ou.edu.vn, henycuong@gmail.com

Duc-Duy Pham
Advanced Structural Engineering Laboratory
Faculty of Civil Engineering
Ho Chi Minh City Open University
Ho Chi Minh City, Vietnam
duy.pd@ou.edu.vn

Thanh-Tuan Tran
Institute of Offshore Wind Energy
Kunsan National University
Kunsan City, Cheollabuk-Do, Republic of Korea
tranthanhtuan@kunsan.ac.kr

Trong Nghia-Nguyen
Faculty of Civil Engineering
Ho Chi Minh City Open University
Ho Chi Minh City, Vietnam
nghia.nt@ou.edu.vn

Abstract—Predicting the behavior of concrete in a Concrete-Filled Steel Tubular (CFST) column is challenging due to the sensitivity to input parameters such as the size of the cross-section, the material modeling, and the boundary conditions. The present paper proposes a new modified finite element model to predict the behavior and strength of a CFST subjected to axial compression. The development is based on the concrete damaged plasticity model, with its stress-strain relationship revised from the available model. The predicted accuracy of the modified model is verified via a wide range of experimental tests. The proposed model has more accuracy than the available models in predicting the ultimate compression strength. The results show good agreement with the test data, allowing its use in modeling CFST columns.

Keywords-CFST columns; axial compression; finite element modeling; stress-strain relationship; steel; concrete

I. INTRODUCTION

Concrete-Filled Steel Tubular (CFST) columns are widely used in modern constructions. Many studies have been conducted in order to understand the behavior of these composite columns, either experimental [1, 2] or analytical [3, 4]. Based on the outcomes from these investigations, different guidelines and codes have been published for the design procedure [5, 6]. CFST columns combined with steel-framed structures [7, 8] form very powerful structures. Authors in [9] used fiber reinforced polymer tubes filled with recycled materials and concrete for pile foundations. Using Finite Element (FE) models has become a popular technique to model CFST via software such as ANSYS and ABAQUS. This approach can model the interaction between concrete core and steel tube accurately. In this study, the FE software ABAQUS is used to FE model CFST. Recently, authors in [10] studied the influence of geometric and material properties on the behavior of the Concrete-Filled Double Skin Steel Tube (CFDST) member with M16 studs under bending. The material model is an input parameter that is mainly affected by the behavior of CFST. Several concrete and steel stress-strain $\sigma-\varepsilon$ models have been developed [11-16]. Almost all models are developed from experimental data based on regression analysis. Authors in [17, 18] proposed FE modeling for analyzing box and circular CFST columns. Authors in [16] developed a simplified model to calculate the capacity of the cross-section and the axial force via the load-deformation $N-\varepsilon$ curve based on 50 test data of Self-Consolidating Concrete (SCC) filled Hollow Structural Steel (HSS) stub columns. Similarly, authors in [14, 15] proposed a simple and effective model for CFST subjected to extreme loadings. In [11], the steel $\sigma-\varepsilon$ relationship was revised based on the available models by [19]. In the present study, the concrete $\sigma-\varepsilon$ curve developed in [12] is revised via the modification of the plateau branch to represent the actual behavior of the material.

This paper aims to develop an FE model of circular CFST columns under axial compression loading. A modified $\sigma-\varepsilon$ model is proposed for the concrete material. The purpose of this study is to improve the accuracy of the FE model using ABAQUS. The accuracy and effectiveness of the new model are verified against the test data from [3, 20]. In the future, focus may be given to the behavior of CFST with steel fiber reinforcement [21], concrete using fly ash [22], or concrete with cement paste including silica oxide nanoparticles.

II. DEVELOPMENT OF THE MATERIAL MODELS

A. Steel Material Model

In this study, the material model proposed in [19] is adopted for the characteristics of the stress-strain curves, as illustrated in Figure 1. The relationship of $\sigma-\varepsilon$ can be expressed as follows:

Corresponding author: Phu-Cuong Nguyen

$$\sigma = \begin{cases} E_s\varepsilon & 0 \le \varepsilon \le \varepsilon_y \\ f_y & \varepsilon_y \le \varepsilon \le \varepsilon_p \\ f_u - (f_u - f_y) \times \left(\frac{\varepsilon_u - \varepsilon}{\varepsilon_u - \varepsilon_p}\right)^p & \varepsilon_p \le \varepsilon \le \varepsilon_u \\ f_u & \varepsilon \ge \varepsilon_u \end{cases} \quad (1)$$

where E_s is Young's modulus of steel, f_y is the yield strength corresponding to the yield strain $\varepsilon_y = \frac{f_y}{E_s}$, f_u is the ultimate strength corresponding to the ultimate strain ε_u, p is the hardening exponent that can be calculated as:

$$p = E_p \times \left(\frac{\varepsilon_u - \varepsilon_p}{f_u - f_y}\right) \quad (2)$$

where E_p is the initial elastic modulus at the onset of strain hardening, and can be taken as $0.02E_s$. Yield strain ε_p and ultimate strain ε_u can be expressed based on the range of yield strength f_y which is 200MPa-800MPa:

$$\varepsilon_p = \begin{cases} 15 \times \varepsilon_y & f_y \le 300 \\ [15 - 0.018(f_y - 300)] \times \varepsilon_y & f_y \ge 300 \end{cases} \quad (3)$$

$$\varepsilon_u = \begin{cases} 100 \times \varepsilon_y & f_y \le 300 \\ [100 - 0.15(f_y - 300)] \times \varepsilon_y & f_y \ge 300 \end{cases} \quad (4)$$

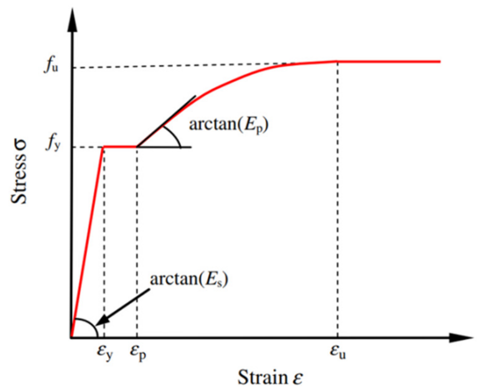

Fig. 1. Constitutive model of steel.

B. Concrete Material Model

Characteristics of stress-strain curves for concrete have been studied in [1, 24]. Most researchers focused on the development of a $\sigma - \varepsilon$ model based on the experimental results. For example, in [25], $\sigma - \varepsilon$ cuves for the fiber model of concrete have been developed to predict the monotonic and cyclic force-deformation behavior of CFST columns. Similar studies have been performed in [2, 26]. In these works, empirical models were proposed for the strain-softening response for CFST. In this paper, the damaged plasticity model of concrete material is utilized. This model is available in ABAQUS and can be easily used by defining some key material parameters. These factors are calibrated and verified with the extensive test results of [27-29] and they are briefly introduced as follows:

Young's modulus of concrete is predicted based on the concrete strength (f_c') [30]:

$$E_c = 4700\sqrt{f_c'} \quad (5)$$

According to [31], the ratio of compressive strength under biaxial loading to the uniaxial compressive strength (f_{b0}/f_c') is obtained based on the available data in the literature as follows:

$$\frac{f_{b0}}{f_c'} = 1.5 \times (f_c')^{-0.075} \quad (6)$$

The fracture energy (G_F) that is defined as the tensile softening response beyond the failure stress, depends on the maximum coarse aggregate size (d_{max}) and concrete strength (f_c'). The following equation can be deduced to determine G_F [32, 33]:

$$G_F = (0.0469 \times d_{\max}^2 - 0.5 \times d_{max} + 26)\left(\frac{f_c'}{10}\right)^{0.7} \quad (7)$$

Authors in [29] stated that the compressive meridian (K_c) that is used to determine the yield surface of the material model, varied in the range from 0.5 to 1, and it is expressed as a function of equibiaxial concrete strength (f_{b0}) and concrete strength (f_c') [34]:

$$K_c = \frac{5.5 \times f_{b0}}{3 \times f_c' + 5 \times f_{b0}} \quad (8)$$

The dilation angle (ψ) factor is used to define the plastic flow potential. This parameter is affected by the confining stress and plastic deformation of the material [27]. The factor ψ is determined as the function of the confinement factor (ξ_c) based on regression analysis [1]:

$$\psi = \begin{cases} 56.3 \times (1 - \xi_c) & \xi_c \le 0.5 \\ 6.672e^{\left(\frac{7.4}{4.64 + \xi_c}\right)} & \xi_c > 0.5 \end{cases} \quad (9)$$

in which the confinement factor is calculated as: $\xi_c = A_s f_y'/A_c f_c'$, where A_s and A_c are the cross-sections of the steel tube and concrete respectively.

For the strain hardening–softening rule, authors in [12] proposed a $\sigma - \varepsilon$ curve for confined concrete through the tests. This model is revised in the present paper. The details of the proposed model are described below.

C. The Proposed Stress-Strain Relationship for Concrete

The $\sigma - \varepsilon$ model developed in [12] is modified to describe the effective $\sigma - \varepsilon$ relationship of confined concrete by the steel tube, as illustrated in Figure 2. The model includes three main stages, corresponding to ascending branch (OA), plateau branch (AB), and descending branch (BC). The initial stage OA is described as follows:

$$\frac{\sigma}{f_c'} = \frac{aX + bX^2}{1 + (a-2)X + (b+1)X^2} \quad \text{if } 0 < \varepsilon \le \varepsilon_{c0} \quad (10)$$

where $X = \frac{\varepsilon}{\varepsilon_{CO}}$, a and b are factors that are defined in (11):

$$a = \frac{E_c\varepsilon_{c0}}{f_c'}, b = \frac{(a-1)^2}{0.55} - 1 \quad (11)$$

The parameter ε_{c0} of the unconfined concrete is expressed based on the regression analysis of over 100 test data from 17 references [35], in which the uniaxial compressive strength f_c' ranges from 10 to 100MPa:

$$\varepsilon_{c0} = 0.00076 + \sqrt{\left(0.626 f_c' - 4.33\right) \times 10^{-7}} \quad (12)$$

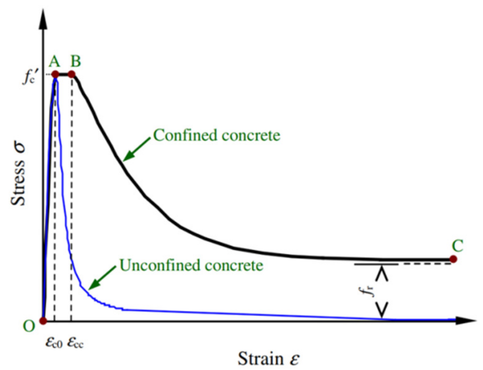

Fig. 2. The constitutive model of confined concrete.

The ultimate strain ε_{cc} of the confined concrete is expressed using the model of [12]. In this model, ε_{cc} depends on the compressive strength f_c', and confining stress at the point B, f_B:

$$\frac{\varepsilon_{cc}}{\varepsilon_{c0}} = e^k$$

$$k = (2.9224 - 0.00367 \times f_c')\left(\frac{f_B}{f_c'}\right)^{0.3124+0.002\times f_c'} \quad (13)$$

It is worth mentioning that the confining stress only happens before and after the yielding location of the material. In this study, the confining stress of the circular column is determined based on the regression analysis as follows:

$$f_B = \frac{1+0.0324\times f_y}{e^{0.0212\times\frac{D}{t}}} \quad (14)$$

The constant value of confining stress f_B remains from ε_{c0} to ε_{cc}' corresponding to the plateau branch (AB) that represents the increment of the peak strain of the concrete due to confinement. For the last stage of the concrete model (BC), the model of [36] is used, which is expressed as follows:

$$\sigma = f_{re} + (f_c' - f_{re}) \times \exp\left[-\left(\frac{\varepsilon-\varepsilon_{cc}}{\alpha}\right)^{\beta}\right] \quad if\ \varepsilon > \varepsilon_{cc} \quad (15)$$

where f_{re} is the residual stress [1] and α and β are factors determining the shape of the softening stage. The parameter β can be taken as 1.2 [1], and α is calculated as follows:

$$\alpha = 0.04 - \frac{0.036}{1+e^{6.08\xi_c - 3.49}} \quad (16)$$

III. Numerical Modeling

A. Finite Element Modeling

The current paper used the available model developed in [37]. The diameter and length of the CFST are 300mm and 900mm respectively. The thickness of the steel tube is 3.2mm. Concrete with 27.2MPa compressive strength and 0.351 of ultimate strain is assigned for the concrete core, while steel with yield strength of 232MPa is assigned for the steel tube.

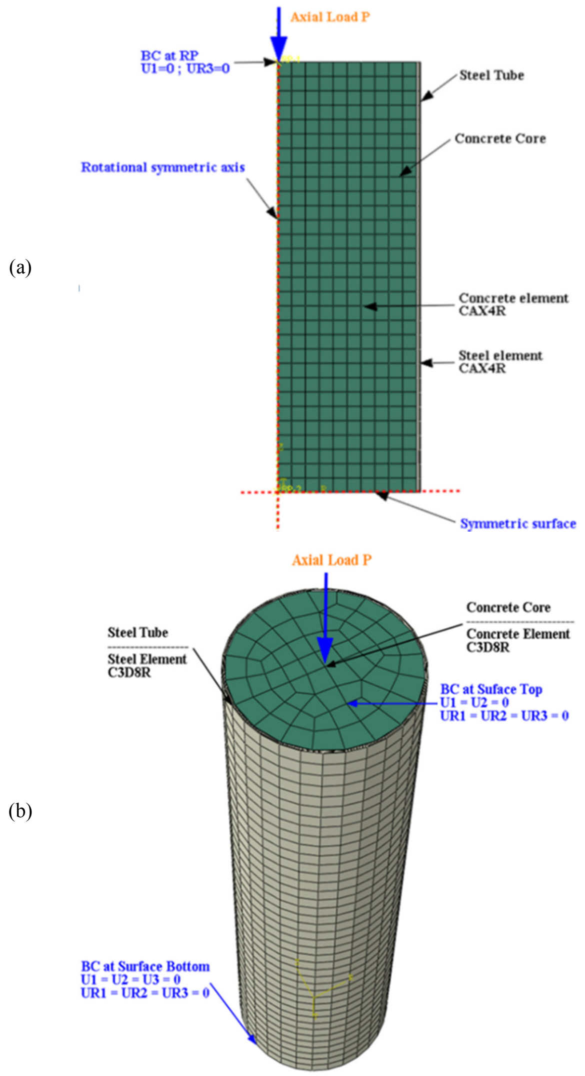

Fig. 3. Modeling of a CFST column. (a) Axisymmetric model, (b) full 3D model.

The finite element model of Figure 3 is developed in ABAQUS. The steel tube and concrete are simulated by a 4-node bilinear element with reduced integration with hourglass control (CAX4R). The mesh size of each element ranges from *D*/20 to *D*/10 which can provide accurate simulation. For the interaction between the steel tube and the concrete core, the surface-to-surface contact with *Hard contact* condition is used to model linear behavior, and the *Column friction model* is used to simulate the nonlinear behavior with a coefficient of 0.6 [3]. For boundary condition, the bottom surfaces are assumed to be fully fixed against all degrees of freedom. The incremental load is applied on the top of the column using the displacement control method to solve.

B. Effect of the Mesh Size on Finite Element Analysis

The accuracy and required computing time of the FE model are investigated in this section. Different meshing approaches, including the axisymmetric model and 3D model, are generated. Figure 4 illustrates the stress distribution from each model under the axial force. It can be seen that there is no obvious effect on the predicted Von Mises stress for the CFST column. For better consideration, the axial load-strain ($N-\varepsilon$) relationship is obtained, as shown in Figure 5. The predicted responses from the two meshing approaches are almost the same as those from the experiment-tested CU-070 [20]. An important finding is that the computational time in the axisymmetric model is only 22sec which is less by a factor of 20 when compared to the 3D model. It can be concluded that the FE axisymmetric model can give accurate and efficient computation.

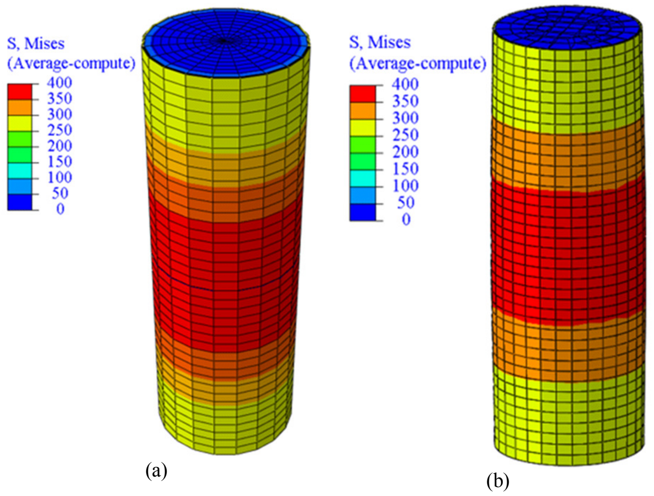

Fig. 4. Stress distribution of different models. (a) Axisymmetric model, (b) full 3D model.

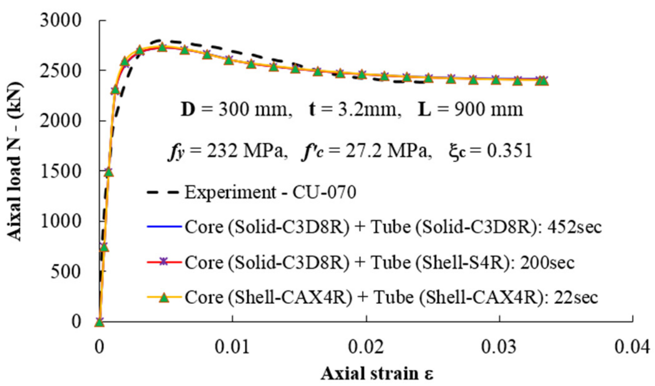

Fig. 5. Influence of the meshing and element types.

IV. VERIFICATION AND DISCUSSION

A. Ultimate Strength

The data of 663 circular CFST columns from the previous studies are selected for validation. The ultimate strength N_u is defined as the peak load of the $N-\varepsilon$ curve. In this paper, the ultimate strength from the proposed model N_u^p is compared with those obtained from the available models in [3, 20]. N_u^p is normalized with the measured ultimate strength N_u^m, which is denoted as N_u^p/N_c^m. The comparison is summarized in Table I. It can be seen that the result obtained from the FE model is more conservative than those produced from the available models. Additionally, the smallest value of standard deviation for the proposed model is found to be 0.055. The results indicate that the predicted outcomes from the current FE model are more reasonable than the previous models.

TABLE I. ULTIMATE STRENGTH OBTAINED FROM THE PROPOSED AND OTHER MODELS

	[3]	[20]	Proposed
Mean	0.975	0.980	1.011
Std.	0.090	0.129	0.055

B. $N-\varepsilon$ Curves of the CFST Column

In terms of the prediction of the $N-\varepsilon$ curves, the proposed model is compared to the available models from [3, 20]. The comparison is performed for different specimens obtained from [2, 16, 20]. Figure 6 illustrates the predicted $N-\varepsilon$ relationship of normal CFST, with its modeling parameters taken from [20]. The observed result from the FE model agrees with the experiment very well.

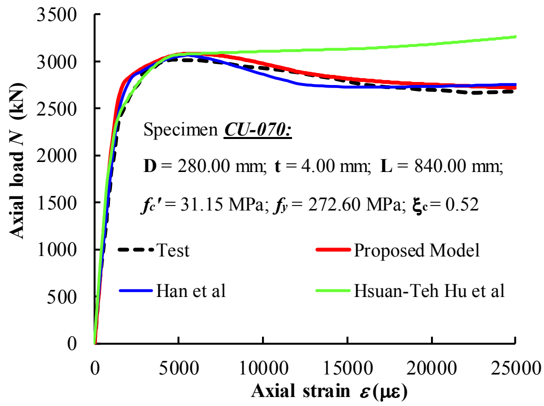

Fig. 6. *N–ε* curves of CFST column for normal specimens.

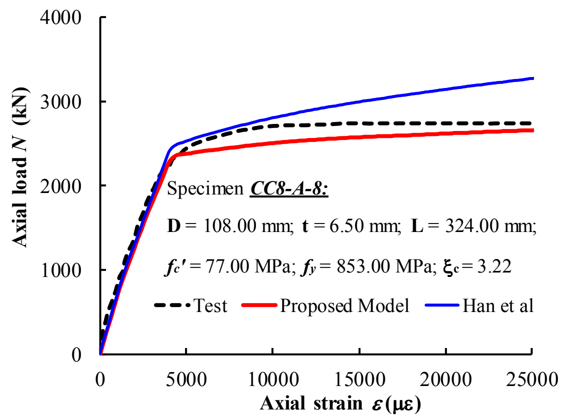

Fig. 7. *N–ε* curves of CFST column with 21.7≤ D/t ≤150.

Figure 7 shows the prediction of the $N-\varepsilon$ curve of the specimen reported in [2]. In this test, the ratio D/t varies from 21.7 to 150. As can be seen, the unsafety in the prediction is obtained for the model in [3] in the post-yielding strength branch. On the contract, the modified FE model gives a better prediction with the test. Furthermore, the predicted $N-\varepsilon$ relationship was also performed for specimens with thin-walled steel tube and high-strength, as shown in Figure 8. The test curve is shown in [16]. The results indicate that the prediction from the FE modeling matches very well with those obtained from Han et al.'s model [16] and the test. In contrast, Hu et al.'s model [20] is an unsafe prediction in the post-yielding strength stage. The above discussion leads to the conclusion that the developed FE model can be used in simulating the CFST column under axial compression for accuracy, effectiveness, and safety predictions.

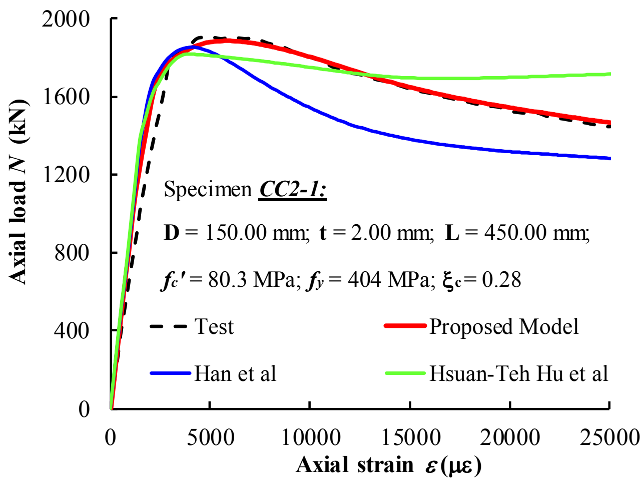

Fig. 8. N–ε curves of the CFST column with thin-walled and high-strength steel.

V. CONCLUSION

The current paper developed a FE modeling for axially loaded circular concrete-filled steel tube columns. The proposed model is compared with the available models in terms of accurate prediction. A new FE model is used to analyze the CFST subjected to axial compression. The model revised the $\sigma-\varepsilon$ curve in [12]. The proposed model is more accurate than the models in [3, 20]. in predicting the ultimate strength. The predicted $N-\varepsilon$ curve from the new model matches well with the test data, for both normal materials and thin-walled steel tubes, which indicates the versatility of the developed modeling in calculating the load-deformation curves. Regarding future work, the behavior of CFST columns with steel fiber reinforcement [21], concrete using fly ash [22], concrete with cement paste with including silica oxide nanoparticles [20], etc. can be studied by performing FEM simulation.

ACKNOWLEDGMENT

The authors gratefully acknowledge the financial support provided by the Scientific Research Fund of Ho Chi Minh City Open University, Vietnam. (No. E2019.02.2).

REFERENCES

[1] Z. Tao, Z.-B. Wang, and Q. Yu, "Finite element modelling of concrete-filled steel stub columns under axial compression," *Journal of Constructional Steel Research*, vol. 89, pp. 121–131, Oct. 2013, https://doi.org/10.1016/j.jcsr.2013.07.001.

[2] K. Sakino, H. Nakahara, S. Morino, and I. Nishiyama, "Behavior of Centrally Loaded Concrete-Filled Steel-Tube Short Columns," *Journal of Structural Engineering*, vol. 130, no. 2, pp. 180–188, Feb. 2004, https://doi.org/10.1061/(ASCE)0733-9445(2004)130:2(180).

[3] L.-H. Han, G.-H. Yao, and Z. Tao, "Performance of concrete-filled thin-walled steel tubes under pure torsion," *Thin-Walled Structures*, vol. 45, no. 1, pp. 24–36, Jan. 2007, https://doi.org/10.1016/j.tws.2007.01.008.

[4] P. K. Gupta, S. M. Sarda, and M. S. Kumar, "Experimental and computational study of concrete filled steel tubular columns under axial loads," *Journal of Constructional Steel Research*, vol. 63, no. 2, pp. 182–193, Feb. 2007, https://doi.org/10.1016/j.jcsr.2006.04.004.

[5] Aci Committee 318, *Building Code Requirements for Structural Concrete (ACI 318-08) and Commentary*. Michigan, USA: American Concrete Institute, 2008.

[6] R. P. Johnson and D. Anderson, *Designers' Guide to EN 1994-1-1: Eurocode 4: Design of Composite Steel and Concrete Structures. General rules and rules for buildings*. London, UK: Thomas Telford, 2004.

[7] P. C. Nguyen, "Nonlinear Inelastic Earthquake Analysis of 2D Steel Frames," *Engineering, Technology & Applied Science Research*, vol. 10, no. 6, pp. 6393–6398, Dec. 2020, https://doi.org/10.48084/etasr.3855.

[8] P. C. Nguyen, B. Le-Van, and S. D. T. V. Thanh, "Nonlinear Inelastic Analysis of 2D Steel Frames : An Improvement of the Plastic Hinge Method," *Engineering, Technology & Applied Science Research*, vol. 10, no. 4, pp. 5974–5978, Aug. 2020, https://doi.org/10.48084/etasr.3600.

[9] V. Farhangi and M. Karakouzian, "Effect of Fiber Reinforced Polymer Tubes Filled with Recycled Materials and Concrete on Structural Capacity of Pile Foundations," *Applied Sciences*, vol. 10, no. 5, p. 1554, Jan. 2020, https://doi.org/10.3390/app10051554.

[10] S.-E. Kim *et al.*, "Finite element simulation of normal – Strength CFDST members with shear connectors under bending loading," *Engineering Structures*, vol. 238, Jul. 2021, Art. no. 112011, https://doi.org/10.1016/j.engstruct.2021.112011.

[11] U. Katwal, Z. Tao, M. K. Hassan, and W.-D. Wang, "Simplified Numerical Modeling of Axially Loaded Circular Concrete-Filled Steel Stub Columns," *Journal of Structural Engineering*, vol. 143, no. 12, Dec. 2017, Art. no. 04017169, https://doi.org/10.1061/(ASCE)ST.1943-541X.0001897.

[12] A. K. Samani and M. M. Attard, "A stress–strain model for uniaxial and confined concrete under compression," *Engineering Structures*, vol. 41, pp. 335–349, Aug. 2012, https://doi.org/10.1016/j.engstruct.2012.03.027.

[13] M. D. Denavit and J. F. Hajjar, "Nonlinear Seismic Analysis of Circular Concrete-Filled Steel Tube Members and Frames," *Journal of Structural Engineering*, vol. 138, no. 9, pp. 1089–1098, Sep. 2012, https://doi.org/10.1061/(ASCE)ST.1943-541X.0000544.

[14] G. D. Hatzigeorgiou, "Numerical model for the behavior and capacity of circular CFT columns, Part I: Theory," *Engineering Structures*, vol. 30, no. 6, pp. 1573–1578, Jun. 2008, https://doi.org/10.1016/j.engstruct.2007.11.001.

[15] G. D. Hatzigeorgiou, "Numerical model for the behavior and capacity of circular CFT columns, Part II: Verification and extension," *Engineering Structures*, vol. 30, no. 6, pp. 1579–1589, Jun. 2008, https://doi.org/10.1016/j.engstruct.2007.11.002.

[16] L.-H. Han, G.-H. Yao, and X.-L. Zhao, "Tests and calculations for hollow structural steel (HSS) stub columns filled with self-consolidating concrete (SCC)," *Journal of Constructional Steel Research*, vol. 61, no. 9, pp. 1241–1269, Sep. 2005, https://doi.org/10.1016/j.jcsr.2005.01.004.

[17] D.-D. Pham and P.-C. Nguyen, "Finite Element Modelling for Axially Loaded Concrete-Filled Steel Circular Tubes," in *CIGOS 2019, Innovation for Sustainable Infrastructure*, C. Ha-Minh, D. V. Dao, F.

Benboudjema, S. Derrible, D. V. K. Huynh, and A. M. Tang, Eds. Singapore: Springer, 2020, pp. 75–80.

[18] D.-D. Pham, P.-C. Nguyen, D.-L. Nguyen, and H.-A. Le, "Simulation of Concrete-Filled Steel Box Columns," in *ICSCEA 2019*, Singapore, 2020, pp. 359–366, https://doi.org/10.1007/978-981-15-5144-4_30.

[19] Z. Tao, X.-Q. Wang, and B. Uy, "Stress-Strain Curves of Structural and Reinforcing Steels after Exposure to Elevated Temperatures," *Journal of Materials in Civil Engineering*, vol. 25, no. 9, pp. 1306–1316, Sep. 2013, https://doi.org/10.1061/(ASCE)MT.1943-5533.0000676.

[20] H.-T. Hu, C.-S. Huang, M.-H. Wu, and Y.-M. Wu, "Nonlinear Analysis of Axially Loaded Concrete-Filled Tube Columns with Confinement Effect," *Journal of Structural Engineering*, vol. 129, no. 10, pp. 1322–1329, Oct. 2003, https://doi.org/10.1061/(ASCE)0733-9445(2003)129:10(1322).

[21] B. Gebretsadik, K. Jdidirendi, V. Farhangi, and M. Karakouzian, "Application of Ultrasonic Measurements for the Evaluation of Steel Fiber Reinforced Concrete," *Engineering, Technology & Applied Science Research*, vol. 11, no. 1, pp. 6662–6667, Jan. 2021, https://doi.org/10.48084/etasr.3915.

[22] M. M. Roshani, S. H. Kargar, V. Farhangi, and M. Karakouzian, "Predicting the Effect of Fly Ash on Concrete's Mechanical Properties by ANN," *Sustainability*, vol. 13, no. 3, Jan. 2021, Art. no. 1469, https://doi.org/10.3390/su13031469.

[23] M. Karakouzian, V. Farhangi, M. R. Farani, A. Joshaghani, M. Zadehmohamad, and M. Ahmadzadeh, "Mechanical Characteristics of Cement Paste in the Presence of Carbon Nanotubes and Silica Oxide Nanoparticles: An Experimental Study," *Materials*, vol. 14, no. 6, Jan. 2021, Art. no. 1347, https://doi.org/10.3390/ma14061347.

[24] L.-H. Han, C.-C. Hou, and Q.-L. Wang, "Behavior of circular CFST stub columns under sustained load and chloride corrosion," *Journal of Constructional Steel Research*, vol. 103, pp. 23–36, Dec. 2014, https://doi.org/10.1016/j.jcsr.2014.07.021.

[25] A. H. Varma, R. Sause, J. M. Ricles, and Q. Li, "Development and Validation of Fiber Model for High-Strength Square Concrete-Filled Steel Tube Beam-Columns," *Structural Journal*, vol. 102, no. 1, pp. 73–85, Jan. 2005, https://doi.org/10.14359/13532.

[26] K. A. S. Susantha, H. Ge, and T. Usami, "Uniaxial stress–strain relationship of concrete confined by various shaped steel tubes," *Engineering Structures*, vol. 23, no. 10, pp. 1331–1347, Oct. 2001, https://doi.org/10.1016/S0141-0296(01)00020-7.

[27] T. Yu, J. G. Teng, Y. L. Wong, and S. L. Dong, "Finite element modeling of confined concrete-II: Plastic-damage model," *Engineering Structures*, vol. 32, no. 3, pp. 680–691, Mar. 2010, https://doi.org/10.1016/j.engstruct.2009.11.013.

[28] J. G. Teng, Y. L. Huang, L. Lam, and L. P. Ye, "Theoretical Model for Fiber-Reinforced Polymer-Confined Concrete," *Journal of Composites for Construction*, vol. 11, no. 2, pp. 201–210, Apr. 2007, https://doi.org/10.1061/(ASCE)1090-0268(2007)11:2(201).

[29] P. E. C. Seow and S. Swaddiwudhipong, "Failure Surface for Concrete under Multiaxial Load—a Unified Approach," *Journal of Materials in Civil Engineering*, vol. 17, no. 2, pp. 219–228, Apr. 2005, https://doi.org/10.1061/(ASCE)0899-1561(2005)17:2(219).

[30] Aci Committee 318, *Building Code Requirements for Structural Concrete and Commentary (ACI 318-11)*. Michigan, USA: American Concrete Institute, 2012.

[31] V. K. Papanikolaou and A. J. Kappos, "Confinement-sensitive plasticity constitutive model for concrete in triaxial compression," *International Journal of Solids and Structures*, vol. 44, no. 21, pp. 7021–7048, Oct. 2007, https://doi.org/10.1016/j.ijsolstr.2007.03.022.

[32] Z. P. Bazant and E. Becq-Giraudon, "Statistical prediction of fracture parameters of concrete and implications for choice of testing standard," *Cement and Concrete Research*, vol. 32, no. 4, pp. 529–556, Apr. 2002, https://doi.org/10.1016/S0008-8846(01)00723-2.

[33] C. E.-I. D. B. Eton, *CEB-FIP Model Code 1990*. London, UK: Thomas Telford Publishing, 1993.

[34] T. Yu, J. G. Teng, Y. L. Wong, and S. L. Dong, "Finite element modeling of confined concrete-I: Drucker–Prager type plasticity model," *Engineering Structures*, vol. 32, no. 3, pp. 665–679, Mar. 2010, https://doi.org/10.1016/j.engstruct.2009.11.014.

[35] B. De Nicolo, L. Pani, and E. Pozzo, "Strain of concrete at peak compressive stress for a wide range of compressive strengths," *Materials and Structures*, vol. 27, no. 4, pp. 206–210, May 1994, https://doi.org/10.1007/BF02473034.

[36] B. Binici, "An analytical model for stress–strain behavior of confined concrete," *Engineering Structures*, vol. 27, no. 7, pp. 1040–1051, Jun. 2005, https://doi.org/10.1016/j.engstruct.2005.03.002.

[37] M.-X. Xiong, D.-X. Xiong, and J. Y. R. Liew, "Axial performance of short concrete filled steel tubes with high- and ultra-high- strength materials," *Engineering Structures*, vol. 136, pp. 494–510, Apr. 2017, https://doi.org/10.1016/j.engstruct.2017.01.037.